






Influence of Inclusion $\text{Sb}_2\text{O}_3/\text{NiO}$ Nanostructures on the Morphological, Microstructural, and Optical Characteristics of PVA Polymeric for Gamma-Ray Shielding Applications

Alaa N. Hadi¹ , Mohanad H. Meteab^{2*} , Musaab Khudhur Mohammed¹ 

¹ Department of Physics, College of Education for Pure Sciences, University of Babylon, Babylon 51002, Iraq

² General Directorate of Education in Babylon Governorate, Ministry of Education, Babylon 51001, Iraq

Corresponding Author Email: mohanad.h.meteab87@gmail.com

Copyright: ©2025 The authors. This article is published by IIETA and is licensed under the CC BY 4.0 license (<http://creativecommons.org/licenses/by/4.0/>).

<https://doi.org/10.18280/rcma.350319>

ABSTRACT

Received: 12 May 2025

Revised: 14 June 2025

Accepted: 26 June 2025

Available online: 30 June 2025

Keywords:

PVA, Sb_2O_3 NPs, NiO NPs, FESEM, optical characteristics, gamma ray shielding

This work describes the steps to make PVA composites with varying amounts of Sb_2O_3 and NiO NPs using the solution casting process. The amounts used are 2.3, 4.6 and 6.9 wt.%. Field Emission-Scanning Electron Microscopy (FE-SEM) showed that the Sb_2O_3 NPs, and NiO NPs were evenly distributed across the PVA polymer matrix. Fourier transform-infrared (FT-IR) study revealed that the Sb_2O_3 and NiO NPs embedded in the polymer matrix interacted with one another. FT-IR research shows that the PVA matrix-polymer and $\text{Sb}_2\text{O}_3/\text{NiO}$ NPs physically interact with one another. As the ratio of Sb_2O_3 and NiO NPs in the PVA increased, the absorption coefficient, and refractive index, also increased. Moreover, a significant reduction of 25.83% in the allowed optical band gap was observed, suggesting improved electronic transition behavior. An indirect electron transition has occurred since the absorbance coefficient is less than 10^4 cm^{-1} . Ultimately, the PVA/ $\text{Sb}_2\text{O}_3/\text{NiO}$ nanocomposites exhibit a high radiation shielding efficiency (RSE) of 18.84% for gamma rays, indicating its promising potential as a protective material. The $\text{Sb}_2\text{O}_3/\text{NiO}$ combination provides an optimal compromise between environmental safety, mechanical flexibility, and radiation attenuation, rendering it a suitable option for non-toxic gamma-ray shielding. Enhancing nanoparticle loading and composite thickness may improve RSE, potentially exceeding that of traditional fillers.

1. INTRODUCTION

Nanocomposites have demonstrated considerable potential in many areas, such microelectronic automobiles, delivery of medicines, detectors, injected molded items, membranes, and packaging supplies, aircraft, coverings, adhesives, fireproofing, medical devices, goods for consumers, and many others [1, 2]. The polymer matrix may be modified to meet specific technical requirements as well as size and shape-dependent nanotechnology attributes that can be utilized. This presents significant opportunities for the advancement of polymer-based nanotechnology. Nanocomposites are structures made of polymer matrix and filled with microscopic phases, such as particles in microfibers or nanosheets. The physical characteristics of these materials are greatly affected by the interactions between the molecules of polymers and the nanofillers [3, 4]. One versatile polymer that finds use in many different sectors is polyvinyl alcohol, or PVA. Their remarkable optical characteristics, low density, and high mechanical quality are the primary determinants of this phenomena. Many products and systems rely on polyvinyl alcohol (PVA), including fuel cells, coatings, medicine delivery systems, and adhesives. Hydroxy-groups on the surface and within PVA form strong hydrogen bonds, which give the substance a high melting point that is almost the same

as its decomposition temperature. Because of this property, PVA is more advantageous to process from aqueous solutions during the melting process [5]. Its usefulness as a therapeutic substance is due to its compatibility with human biology [6]. In addition, PVA shows a distinct ability to absorb metal ions, such as mercury, palladium, and copper. The chemical formula for polyvinyl alcohol (PVA) is $(\text{C}_2\text{H}_4\text{O})_x$. The substance possesses a melting point of 230°C and a density from 1.19 into 1.31 g/cm^3 . When temperatures are above 200°C , this thermoplastic polymer begins to decompose. The presence of C-O-C bonds in this material influences its flexible structure. Additionally, it may solubilize in organic solvents, engage with water, exhibit a crystalline structure, and has self-lubricating characteristics [7]. Nanomaterials have garnered considerable interest over the years because of their numerous unique and distinctive properties, including size effects, extensive surface area, high strength, and quantum effects [8].

Antimony oxide (Sb_2O_3) nanoparticles, a crucial metal-oxide composite, have garnered significant interest owing to their enhanced properties relative to the bulk material [9]. It was commonly employed as a fire retardant [10], substance for electrodes [11], catalytic agent [12], chemically sensitive materials, and semiconductor materials [13]. Other industries that make use of it include ceramics, magnetics, rubber, textiles, and aerospace. Synthesis of Sb_2O_3 nanoparticles has

been the focus of most recent efforts. Chemical techniques were employed [14], vacuum vaporization [15], thermal combustion [16], hybrid initiation, and glass heating [17], hydrothermal method [18], and gamma ray radiation-oxidization [19].

Nickel oxide (NiO) is well-defined oxide that crystallizes in a cubic structure. It is a p-type semiconductor with a large indirect band gap (3.6-4.0) eV. The six locations for both nickel and oxygen atoms lead the NiO crystal lattice to mimic NaCl, sometimes known as the rock salt structure [20]. NiO is a strong antiferromagnetic semiconductor with catalytic, gas sensing, and electrochemical applications. Various applications utilize its nanoparticles due to its mechanical, magnetic, electrical, and optical properties. These include catalysts, electrochromic pictures, and fuel cell electrodes [21].

There are two types of radiation that are present in our environment: those that originate from radioactive chemicals that are found naturally on Earth and those that originate from cosmic radiations that arrive from space. Radiation is an indispensable component in a wide variety of businesses in the modern era, including manufacturing and radiation-based treatment. Radiotherapy, radiation diagnostics, and radiation surgery are all functions that fall under the purview of medical technology [22].

However, radiation can be harmful to humans and animals, with larger doses resulting in tissue damage, radiation sickness, and cancer. As a result, radiation shielding has become of critical importance, where lowering the quantity of harmful radiation leads to minimizing the health risk [23, 24].

The inclusion of antimony oxide (Sb_2O_3) and nickel oxide (NiO) nanoparticles inside the PVA matrix markedly enhances the optical and gamma-ray shielding properties of the nanocomposite. Sb_2O_3 , being a relatively high atomic number ($Z = 51$), functions as a primary attenuator of ionising radiation by photoelectric absorption. NiO facilitates radiation scattering and enhances the stability of the polymer structure. The dual inclusion produces a synergistic interaction: Sb_2O_3 enhances shielding efficacy, whereas NiO augments mechanical reinforcement and interfacial adhesion [25].

The amalgamation of Sb_2O_3 and NiO diminishes the optical band gap by generating localised energy levels and interfacial polarisation. This is evidenced by a decrease in both permissible and forbidden indirect band gaps, signifying enhanced photon absorption and altered charge transfer dynamics. The homogeneous distribution and robust interaction of nanoparticles with PVA chains enhance the composite's dielectric properties, rendering it more suitable for flexible optoelectronic devices and radiation-shielding films [25, 26].

The literature encompasses findings from previous investigations on Polymer nanocomposites [27]. synthesized graphene copper ferrite incorporated in PVA for use in optoelectronic devices [28]. The doping with Ag/ TiO_2 enhances the electrical and dielectric properties of a PVA-PVP polymeric mix used in capacitor applications [29]. Enhanced the optical conductivity of the PVA-PVP polymeric mix by using Co_3O_4 nanoparticles [30]. His studies indicate that the incorporation of 2% Co_3O_4 into the matrix elevated its optical bandgap from 5.25 eV to 4.03 eV and enhanced its conductivity from $4.47 \times 10^{-8} \text{ S.cm}^{-1}$ to $3.67 \times 10^{-5} \text{ S.cm}^{-1}$. CuO nanoparticle-based polymer nanocomposites combined with a graphene-PVA mix exhibited significant resistance to gamma irradiation [31]. The ZnO doping enhanced the optical

characteristics of a PVA-PVP polymeric mix for optical limiting applications [32]. The integration of rare-earth elements into PVA enhanced its radiation shielding capabilities [33].

This paper presents the preparation of the PVA/ Sb_2O_3 /NiO nanocomposite and examines its morphological, microstructural, optical characteristics, and their application for the gamma ray attenuation.

2. MATERIALS AND METHODS

In order to assist the dissolving of the 100% (1gm) of polyvinyl alcohol (PVA) in 70 mL of distilled water for 30-minute minutes at temperatures ranging from 75°C to 80°C using a magnetic stirrer. Then, PVA was combined with Sb_2O_3 and NiO nanoparticles at concentrations of (97.7% PVA and 2.3% Sb_2O_3 /NiO), (95.4% PVA and 4.6% Sb_2O_3 /NiO) and (93.1% PVA and 6.9 % Sb_2O_3 /NiO) at temperature 75°C using magnetic stirrer for 1 hours for each added until too homogenous with the PVA polymer to produce nanocomposite films. The solution was then cast into clean, leveled glass Petri dishes and allowed to dry at room temperature for 48 hours, followed by additional drying in a vacuum oven at 50 °C for 6 hours to remove residual moisture. The dried nanocomposite films were carefully peeled and stored in desiccators prior to characterization. The films produced exhibit a thickness of approximately 9 μm . The analysis of the structure at room temperature was conducted using FT-IR (Bruker company, model Vertex-70 spectrometer, German origin), covering the range of (4000-600) cm^{-1} . Researchers utilized a FE-SEM (INSPECT S50, originating from Japan, type FEI-Customer ownership) to analyze the film surface morphology. The Shimadzu UV-1650 PC spectrophotometer from Phillips was utilized to investigate the formation of nanocomposites within the wavelength from (200) nm to (1100) nm.

3. RESULTS AND DISCUSSION

FE-SEM was used to examine the distribution of nanoparticles within the polymer matrix, enabling us to confirm the influence of (Sb_2O_3 /NiO) NPs on the properties of the nanocomposite. Figure 1 shows FE-SEM photographic of PVA/ Sb_2O_3 /NiO nanocomposites films at (20 KX) magnification and a scale of 4 μm , showing the distribution of nanoparticles at different concentrations. Image (a) shows a smooth and homogeneous polymer surface, demonstrating the success of the preparation method. Images (b, c, and d) clearly highlight the dispersion of (Sb_2O_3 /NiO) NPs within the polymer matrix, with an increase in grain size as the nanoparticle concentration increases, reflecting the homogeneous and efficient distribution of these particles within the composite material [34].

FT-IR spectroscopy was employed to examine the chemical characteristics of the newly synthesized nanocomposite of polyvinyl alcohol (PVA) with Sb_2O_3 NPs and NiO NPs across the frequency range of 600 to 4000 cm^{-1} , as seen in Figure 2.

All samples exhibit a prominent absorption band at 3271 cm^{-1} [35], indicative of O-H stretching vibrations. This band is distinct and vivid in the pure PVA spectra, indicating robust intermolecular hydrogen bonding among PVA chains. The incorporation of Sb_2O_3 /NiO nanoparticles (2.3 wt.%, 4.6 wt.%,

and 6.9 wt.%) expands and displaces the band, suggesting the formation of supplementary hydrogen bonds or coordination interactions between the hydroxyl groups of PVA and the surface atoms of the metal oxide. This evidently demonstrates interfacial contact and possible complexation.

Symmetric stretching vibrations of the C–H bond were found at 2938.09 cm^{-1} . A vibrational band at 1732.03 cm^{-1} is also seen, attributed to the stretching of the C=O bond. A distinctive absorption band at 1562.23 cm^{-1} was discovered, attributable to the stretching vibrations of the amine group in chitosan. C-H bond bending vibrations were found at 1432.42 cm^{-1} . The spectral peak at 1241.32 cm^{-1} was utilized to evaluate the material's crystallinity, as indicated in references [36, 37]. The crystalline arrangement of polymer chains is the principal determinant of peak magnitude in spectroscopic investigation. Prior research indicates that a peak size maximum [38, 39] is ascribed to the symmetrical stretching pattern of carbon-carbon bonds or carbon-oxygen bonds within a particular segment of the polymer chain [40]. In this area, two hydroxyl (OH) groups are positioned next to one another on each side of the carbon chain plane, resulting in intramolecular hydrogen bonding. A frequency of 1086.42 cm^{-1} was employed to detect C-O bond vibrations, whereas the pronounced twisting of the C-O-C bond induces vibrations at 846.01 cm^{-1} , and the mild bending vibrations of the C=C bond manifest at 622.19 cm^{-1} . These vibrations indicate the structural and mechanical connections within polymer molecules and enhance the comprehension of their physical characteristics [41].

The nanocomposite spectra continue to exhibit peaks around 2920 cm^{-1} (C-H stretching), $1730\text{--}1650\text{ cm}^{-1}$ (C=O, and H-O-H bending), and 1089 cm^{-1} (C-O-C stretching), albeit with diminished intensity or slight changes. This indicates that the nanoparticles engage in chemical interactions with the polymer chains instead than merely physically blending them. The distinctive spectrum changes seen in this work indicate that the combination of Sb_2O_3 and NiO enhances shielding effectiveness while also influencing the polymer's microstructure and bonding environment. These interactions are anticipated to enhance the optical performance, mechanical properties, and thermal stability of the nanocomposite.

The addition of trace amounts of antimony oxide ($\text{Sb}_2\text{O}_3/\text{NiO}$) at (2.3, 4.6, and 6.9) wt.% by weight ratios within the PVA polymer matrix resulted in significant changes in the intensity of some spectra and shifts at other locations in the infrared spectroscopy. The alterations signify the interaction between the introduced nanoparticles and the polymer matrix, demonstrating the existence of a relationship between the added substances and the polymer structure. FT-IR research demonstrated interactions between the PVA matrix and the ($\text{Sb}_2\text{O}_3/\text{NiO}$) NPs, therefore elucidating the structural impact of these additions on polymer characteristics. These findings align with prior research in this domain [42].

Figure 3 shows the wavelength-dependent changes in absorbance of the PVA/ $\text{Sb}_2\text{O}_3/\text{NiO}$ nanocomposites. The results show that all samples exhibit greater UV absorption compared to pure PVA. At a wavelength of 200 nm, high energy levels cause the donor electrons to transition to the conduction band. Electrons absorb a photon of designated energy to elevate their energy level. As the contribution ratios of ($\text{Sb}_2\text{O}_3/\text{NiO}$) nanoparticles escalated from (0%) to (6.9%), an enhancement in absorbance was noted. At extended wavelengths, the energy of the incoming photons is inadequate

to engage with the atoms, permitting them to traverse without absorption [43, 44].

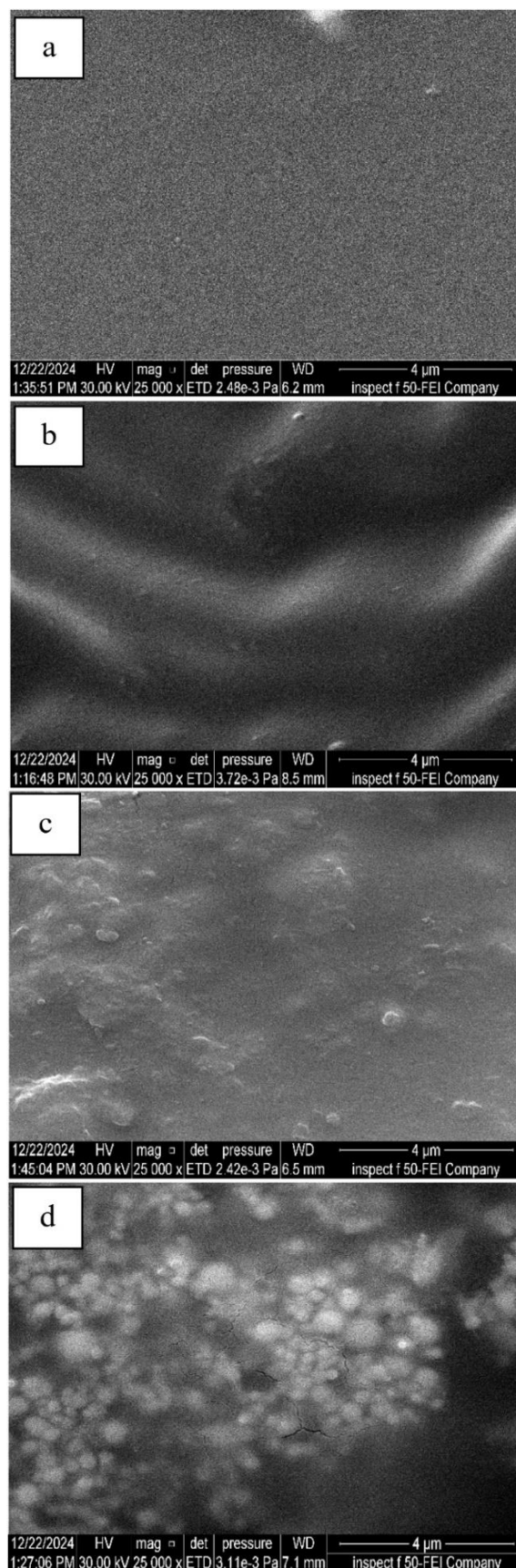


Figure 1. FESEM images for the (a) pure PVA, (b) 2.3 wt.% Sb_2O_3 and NiO NPs, (c) 4.6 wt.% Sb_2O_3 and NiO NPs and (d) 6.9 wt.% Sb_2O_3 and NiO NPs

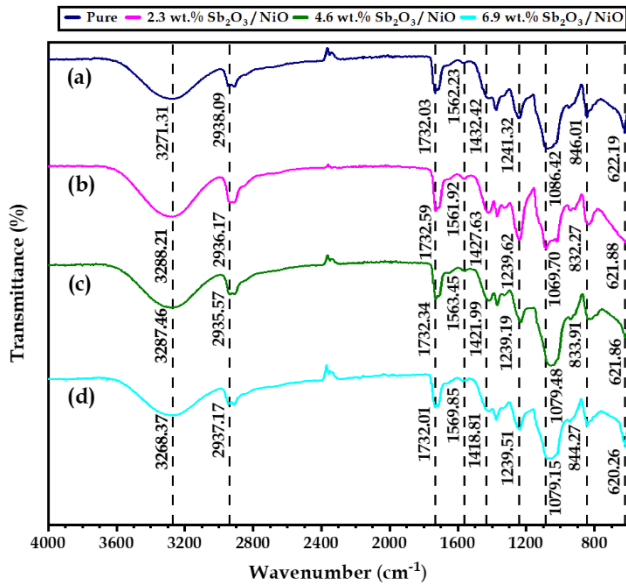


Figure 2. FT-IR spectrum for the (a) Pure-PVA, (b) 2.3 wt.% Sb₂O₃ and NiO NPs, (c) 4.6 wt.% Sb₂O₃ and NiO NPs and (d) 6.9 wt.% Sb₂O₃ and NiO NPs

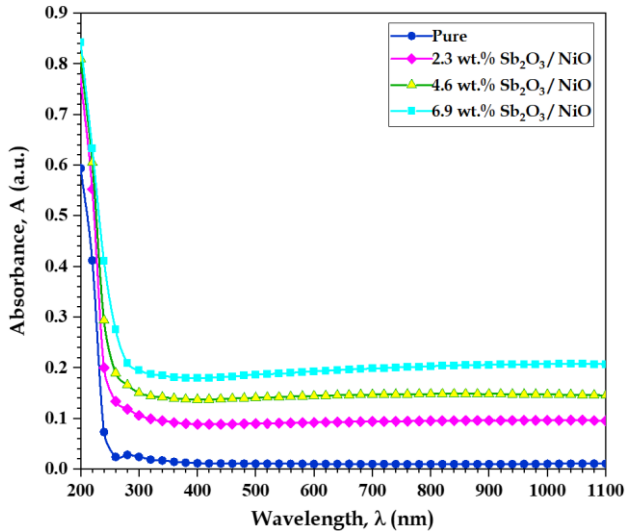


Figure 3. The absorbance of PVA/Sb₂O₃/NiO nanocomposite with wavelength

The transmittance (T) given by the relation [45]:

$$T = e^{-\alpha t} \quad (1)$$

where, α represents the absorption coefficient and t denotes the film thickness. The transmittance, (T) spectrum of PVA/Sb₂O₃/NiO nanocomposites at various wavelengths is depicted in Figure 4, indicating that optical transmittance escalates with increasing wavelength, especially at 260 nm, where a consistent rise in transmittance is noted. The research indicated that antimony oxide (Sb₂O₃) and nickel oxide (NiO) nanoparticles diminish the transmission of light through the material. Furthermore, increasing the concentration of these nanoparticles within the PVA polymer matrix enhances light absorption, which is reflected in a decrease in optical transmittance. These results are consistent with previous research [46].

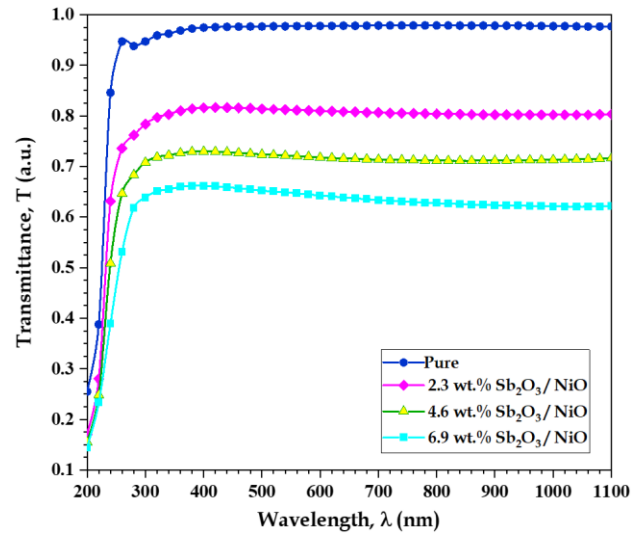


Figure 4. The transmittance of the PVA/Sb₂O₃/NiO nanocomposite as a function of wavelength

The below equation was employed to get the absorption coefficient [47].

$$\alpha = 2.303 \frac{A}{t} \quad (2)$$

A is absorption. Figure 5 illustrates the correlation between photon energy and the absorption coefficient (α) for PVA/Sb₂O₃/NiO nanocomposite films. The absorption coefficient progressively rises with increasing photon energy until it attains 4.78 eV. At this energy, the photon lacks sufficient energy to facilitate the passage of an electron from the valence band to the conduction band due to the minimal electron transition energy. At 4.78 eV, the absorbance coefficient for all samples markedly rises, signifying substantial alterations in the conduction band electrons. The reduction in the absorption coefficient signifies indirect electron transmission since the absorption value is below 10^4 cm^{-1} , indicating indirect electron transport inside the material [48].

The connection was used to calculate the refractive index (n) [49].

$$n = \frac{1 + \sqrt{R}}{1 - \sqrt{R}} \quad (3)$$

where, reflectance is represented by R. Figure 6 illustrates the refractive index curves of PVA/Sb₂O₃/NiO nanocomposites exhibiting significant variations concerning wavelength. When Sb₂O₃ and NiO particles were added to the polymer, an increase in the refractive index values of the sample was observed. This is due to the interaction of these particles with oscillating electromagnetic fields, which leads to electron binding and an enhanced refractive index. Augmenting the concentration of Sb₂O₃ and NiO particles further elevates the refractive index due to the enhancement of the interaction between electrons and the electromagnetic field. This phenomenon aligns with the findings of prior investigations in this domain [50].

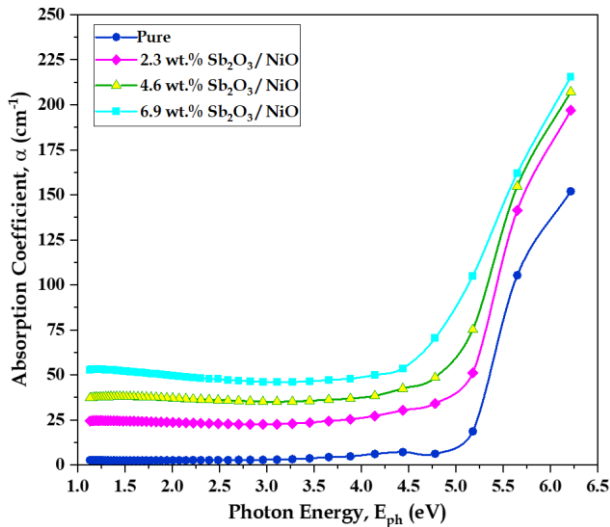


Figure 5. The absorption coefficient of the PVA/Sb₂O₃/NiO nanocomposite as a function of photon energy

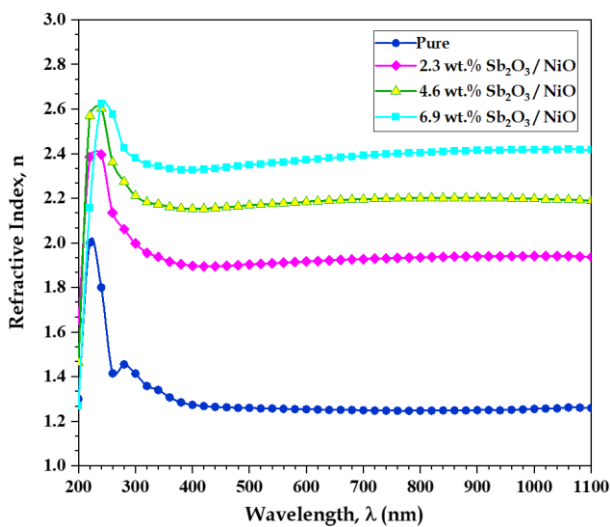


Figure 6. The refractive index of PVA/Sb₂O₃/NiO nanocomposite with wavelength

The indirect energy gap is given by [51]:

$$(\alpha h\nu)^{\gamma} = \beta(h\nu - E_g) \quad (4)$$

For a fixed β , the connections among photon energy ($h\nu$), energy gap (E_g), and the permitted and prohibited indirect transitions ($m=1/\gamma$) may be represented by the numbers 2 and 3. To ascertain the band gap energy (E_g), create a graph that links the absorption coefficient ($\alpha h\nu$) with the photon energy ($h\nu$). If an indirect electron transition is permitted or prohibited, the variable (m) in this equation may take on the values of (1/2) or (1/3). The linear portions of these equations, when extrapolated to the $h\nu$ axis, yield the optical band gap values displayed in Table 1.

Figures 7 and 8 depict the indirect band gaps of pure PVA and the PVA/Sb₂O₃/NiO nanocomposites. With the increasing concentration of (Sb₂O₃/NiO) nanoparticles within the PVA matrix, a gradual decrease in the optical band gap values was observed. The indirect allowed band gap decreased from 4.84 to 3.59 eV, while the indirect forbidden band gap contracted from 4.65 to 2.82 eV. This reduction indicates the influence of nanofiller incorporation in modifying the electronic structure

of the polymer, thereby enhancing light absorption and charge carrier transport within the nanocomposite material.

The results of this study are depicted in Figure 9, which depicts the values of Tauc plots for the permissible and forbidden band gaps of pure PVA as well as the PVA nanocomposites that comprise (Sb₂O₃/NiO). The presented data were further supported by statistical analysis, which included the calculation of standard deviations (SD), standard errors (SE), and error bars for each sample. This validated the reliability of the results and demonstrated that there was a consistent downward trend in the band gap values as the nanoparticle content increased.

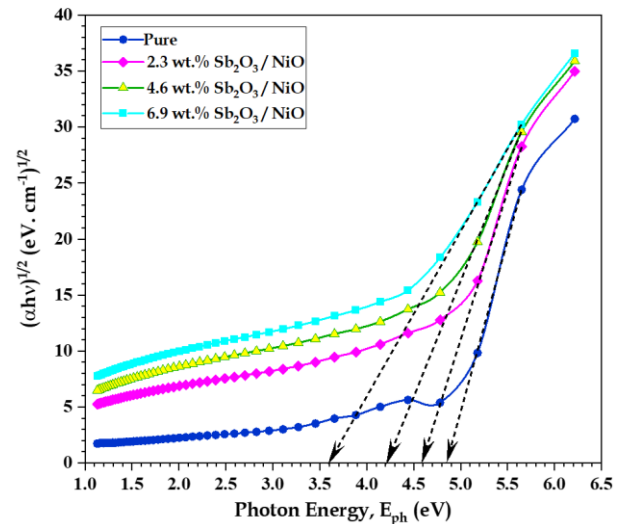


Figure 7. PVA/Sb₂O₃/NiO nanocomposites of $(\alpha h\nu)^{1/2}$ versus $(h\nu)$ as a function of wavelength

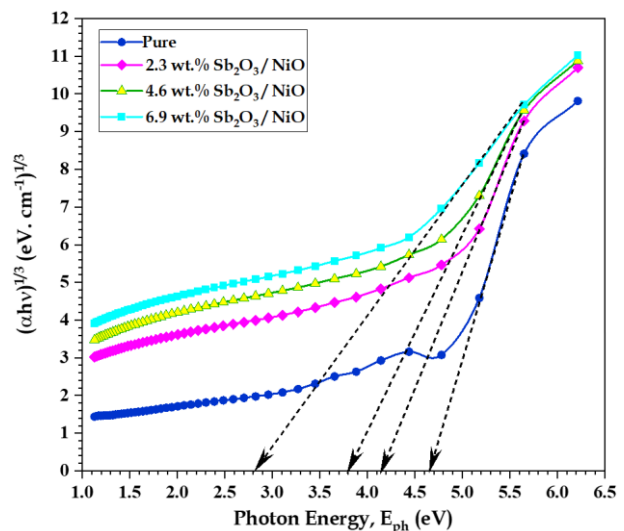


Figure 8. PVA/Sb₂O₃/NiO nanocomposites of $(\alpha h\nu)^{1/3}$ vs. $(h\nu)$ with wavelength

This result primarily arises from uniform nanoparticle distribution and robust interfacial interactions between the inorganic fillers and the polymer matrix. The incorporation of Sb₂O₃ and NiO NPs into the PVA matrix creates localised energy states within the band structure, facilitating electronic transitions at reduced photon energies. This results in a reduction of the band gap.

In addition to this, the nanoscale dispersion of these metal oxides optimises the surface area and improves the

interactions between the nanoparticles and the polymer chains. Interfacial interactions, particularly those that occur at the molecular level, have the potential to result in the formation of localised charge transfer complexes or defect states, both of which have the ability to significantly alter the electrical structure of the composite. There is a common association between these effects and tail states in the band structure. These tail states facilitate optical transitions at reduced excitation energy, which ultimately results in a decrease in the reported optical band gap.

Furthermore, Sb_2O_3 nanoparticles and NiO nanoparticles have inherent semiconducting characteristics, and the insertion of these elements may have an effect on the chain arrangement and crystallinity of the polymer. A reduction in the band gap is made possible as a result of this modification to the microstructure of the polymer. This modification promotes delocalised states and enhances charge transport channels [52, 53].

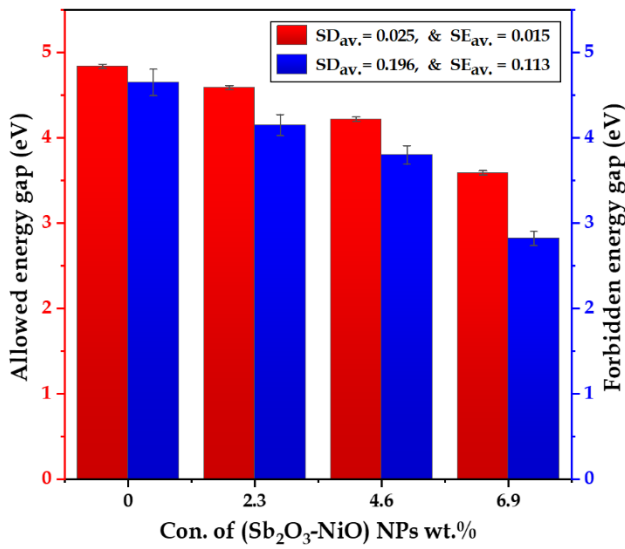


Figure 9. Analysis of indirect allowed and forbidden band gaps of pure PVA and PVA/ Sb_2O_3 /NiO nanocomposites

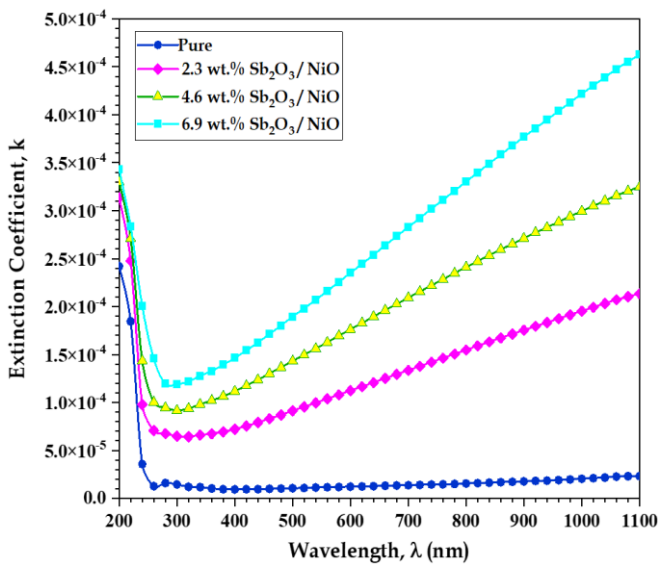


Figure 10. Extinction coefficient of PVA/ Sb_2O_3 /NiO nanocomposite with wavelength

The relation gives the extinction coefficient (k_o) [54]:

$$k_o = \frac{\alpha \lambda}{4\pi} \quad (5)$$

Table 1. PVA/ Sb_2O_3 /NiO nanocomposite permissible and forbidden energy gap values with wavelength

Sb ₂ O ₃ and NiO wt.%	Optical Energy Gap	
	Allowed	Forbidden
0.0	4.84±0.015	4.65±0.136
2.3	4.59±0.015	4.15±0.124
4.6	4.22±0.015	3.80±0.110
6.9	3.59±0.015	2.82±0.084

For each of the films under consideration, Figure 10 displays the correlation between wavelength and absorption coefficient. The PVA/ Sb_2O_3 /NiO nanocomposites' absorption coefficient seems to peak at low energies, namely at 240 nm, and subsequently drop at 260 nm. There is a linear relationship between the Sb_2O_3 /NiO nanoparticle ratio and the absorption coefficient beyond 260 nm. The rise in photon energy explains this trend. In addition, the absorption coefficient of the nanocomposites is positively correlated with the concentration of Sb_2O_3 /NiO particles, which improves the composites' ability to absorb light [55].

The dielectric constant has two parts: real (ϵ_1) and imaginary (ϵ_2) [56]:

$$\epsilon_1 = n^2 - k^2 \quad (6)$$

$$\epsilon_2 = 2nk \quad (7)$$

Figures 11 and 12 depict the fluctuations in the real (ϵ_1) and imaginary (ϵ_2) dielectric constants of PVA/ Sb_2O_3 /NiO nanocomposites, respectively. Pure-PVA has elevated real and imaginary dielectric constant values at shorter wavelengths, which diminish as the wavelength rises. Conversely, energy levels significantly decrease when wavelength diminishes due to the increase in both the real and imaginary dielectric constants of nanocomposite films. The refractive index is more significant in calculating the effective dielectric constant than the absorption coefficient, as the latter is considerably lower, particularly when squared, than the refractive index [57].

The optical conductivity (σ_{op}) is definite by [58]:

$$\sigma_{op} = \alpha nc/4\pi \quad (8)$$

where, c represents the velocity of light. Figure 13 displays the optical conductivity of the PVA/ Sb_2O_3 /NiO nanocomposites. The optical conductivity of the PVA polymer shows a high increase at short wavelengths and a decrease at long wavelengths. This behavior can be explained by the increased absorption coefficient at these wavelengths. It was also observed that the concentration of (Sb_2O_3 /NiO) nanoparticles is directly related to the increase in optical conductivity as a result of the higher absorption coefficients associated with the higher concentration of these particles. This indicates that increasing the nanoparticle concentration enhances phototransistor charge transport within the composite, thereby increasing its optical conductivity [59].

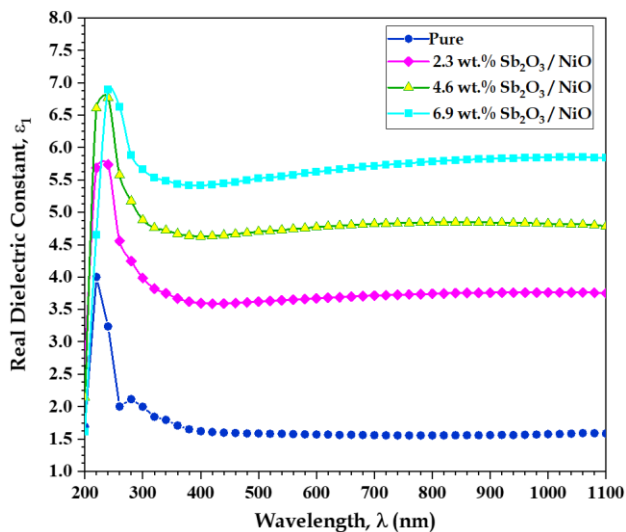


Figure 11. The real dielectric constant of the PVA/Sb₂O₃/NiO mixture is given by the wavelength

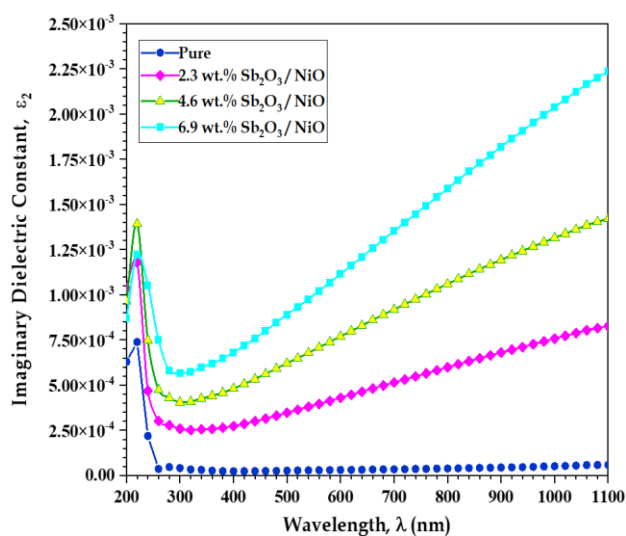


Figure 12. Imaginary dielectric constant of PVA/Sb₂O₃/NiO nanocomposite as a function of wavelength

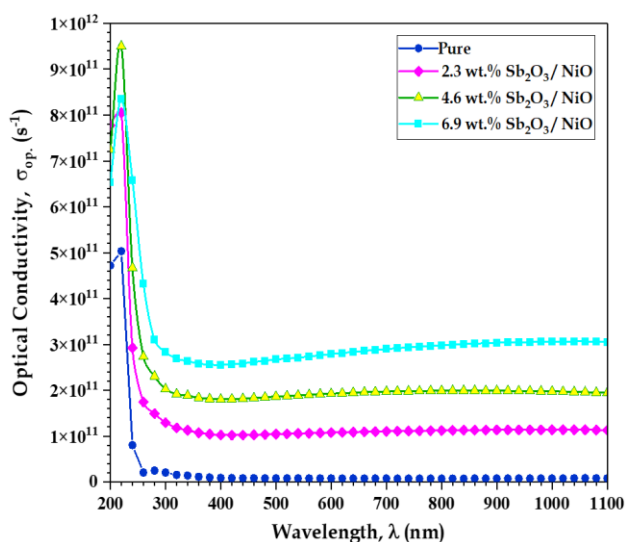


Figure 13. The real dielectric constant of the PVA/Sb₂O₃/NiO mixture is given by the wavelength

The following equation, which is related to the thickness of the absorbing material, can be used to calculate the linear attenuation coefficient (μ) [60]:

$$N/N_0 = e^{-\mu t} \quad (9)$$

In this context, N_0 denotes the count of radiation particles detected during a designated time frame without any absorber, whereas N signifies the count of particles identified in the same time frame after traversing a material of thickness t . The value μ represents the linear attenuation coefficient of gamma radiation. Figure 14 depicts the influence of nanoparticles on the gamma ray attenuation graph, demonstrating the variation in the (N/N_0) ratio with varying quantities of Sb₂O₃/NiO particles incorporated into the PVA polymer matrix. The reduction in radiation transmission with higher concentrations of Sb₂O₃/NiO particles is attributed to the material's enhanced capacity to absorb and attenuate radiation, resulting in less intensity of radiation passing through the sample [61]. Figure 15 shows how the gamma radiation attenuation coefficients are affected by the concentration ratio of (Sb₂O₃/NiO) NPs. The attenuation coefficients increase as the quantity of nanoparticles rises. This is because the shielding materials included inside the nanoparticles enhance the effectiveness of the shielding by absorbing or reflecting gamma radiation. The elevated atomic numbers of both Sb₂O₃ and NiO lead to the maximum attenuation coefficient values seen in polymer nanocomposites containing these particles. Consequently, augmenting the Sb₂O₃/NiO level in the nanocomposite markedly improves its radiation shielding efficacy [62]. In comparison to other frequently utilised fillers, including bismuth oxide (Bi₂O₃), tungsten oxide (WO₃), and lead oxide (PbO), which generally exhibit RSE values between approximately 12% and 25% based on filler concentration and incident radiation energy, the Sb₂O₃/NiO system emerges as a viable alternative. Despite lead oxide's exceptional attenuation properties attributed to its elevated atomic number and density, its toxicity restricts its extensive use. Although lead is the most efficient material for gamma-ray attenuation, it presents considerable environmental and health hazards and is inflexible. The PVA/Sb₂O₃/NiO nanocomposite provides a non-toxic, lightweight, and flexible option, rendering it suitable for wearable and low-to-moderate shielding applications. Through ongoing enhancement of nanoparticle incorporation and thickness, these nanocomposites could significantly contribute to advanced radiation protection technologies [63].

PVA/Sb₂O₃/NiO nanocomposites exhibit significant radiation shielding potential and environmental advantages; nonetheless, some limitations may hinder their extensive practical implementation. The environmental stability of the composite is a primary concern. Polyvinyl alcohol (PVA), a hydrophilic polymer, is very vulnerable to humidity and moisture, which may lead to a decline in the material's performance and structural integrity over time. This limits its use in high-humidity or outdoor environments without further surface treatment or encapsulation. Furthermore, the incorporation of NiO and Sb₂O₃ nanoparticles enhances the composite's shielding effectiveness; nevertheless, it may compromise mechanical strength and flexibility at elevated filler concentrations, leading to brittleness or suboptimal film-forming properties.

Moreover, as agglomeration can diminish the material's overall effectiveness and consistency, achieving uniform

dispersion of nanoparticles inside the polymer matrix remains a significant challenge. A further concern from a production perspective is scalability. When stringent regulation of nanoparticle dispersion and loading is required, solution casting and laboratory-scale synthesis techniques are typically not directly suitable for industrial-scale production. Moreover, unless specifically designed for mass manufacturing, the costs associated with high-purity nanofillers and processing machinery may limit economic viability. Consequently, despite the appeal of PVA/Sb₂O₃/NiO composites as alternatives to conventional materials, their effective and sustained application in radiation shielding technologies hinges on addressing these challenges via composite manufacturing methods, protective coatings, and advanced formulations.

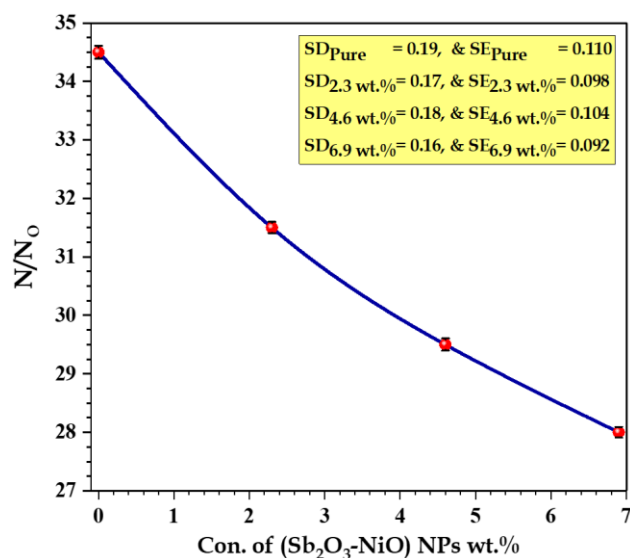


Figure 14. Variation of (N/N_0) for (PVA/Sb₂O₃/NiO) nanostructures

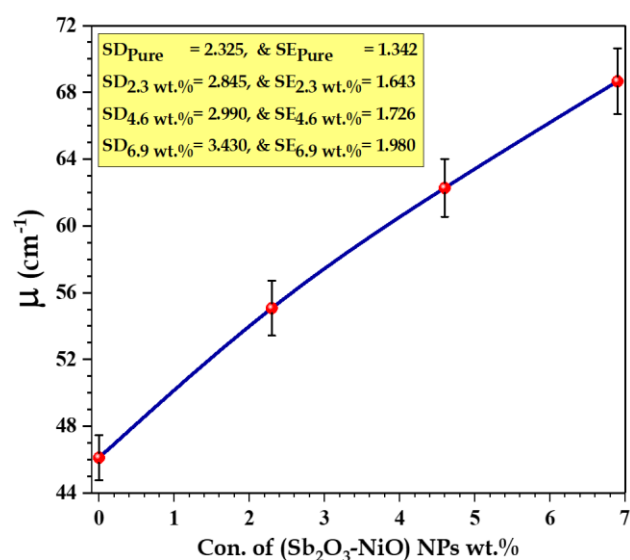


Figure 15. Variation of attenuation coefficients of gamma radiation for (PVA/Sb₂O₃/NiO) nanostructures

4. CONCLUSIONS

In this research, a highly effective method for fabricating

nanocomposites composed of polyvinyl alcohol (PVA) with antimony (Sb₂O₃) and nickel (NiO) oxides using a casting technique is demonstrated. High-resolution scanning electron microscopy (FE-SEM) analyses revealed a homogeneous distribution of antimony and nickel oxide particles within the polymer matrix. (FT-IR) spectroscopy studies also revealed interactions between the various oxide particles and the polymer matrix, indicating physical bonding between the components. As the percentage of (Sb₂O₃/NiO) oxides in the polymer increased, the absorption and extinction coefficients increased, along with the refractive index and the real and effective band gaps. Conversely, the transmittance and indirect band gap decreased, indicating the occurrence of indirect electron transfer. The indirect allowed and forbidden energy gap decreased of 5.17% and 10.75% compared with pure PVA when added 2.3% for Sb₂O₃/NiO NPs, respectively. Finally, PVA/Sb₂O₃/NiO nanocomposites showed high attenuation capacity when exposed to gamma rays. The PVA/Sb₂O₃/NiO nanocomposite exhibited a significant gamma-ray shielding efficiency (RSE) of 18.84%, exceeding that of numerous traditional single-oxide polymer fillers at similar loadings. The results demonstrate a synergistic interaction between Sb₂O₃ and NiO nanoparticles, which collectively improve optical and shielding performance while maintaining the lightweight and flexible characteristics of the polymer matrix. Consequently, the PVA/Sb₂O₃/NiO nanocomposites represent a viable multifunctional material platform for radiation shielding applications, particularly in wearable protective gear and medical settings. Flexible optoelectronic devices necessitate tunable optical band gaps and enhanced dielectric properties, as well as low-toxicity alternatives to lead-based shielding materials, in order to satisfy environmental and safety requirements.

ACKNOWLEDGMENT

The authors express their profound gratitude to the College of Education for Pure Sciences, University of Babylon, Iraq, for offering the requisite facilities.

REFERENCES

- [1] Sharma, S.K., Prakash, J., Sudarshan, K., Sen, D., Mazumder, S., Pujari, P.K. (2015). Structure at interphase of poly (vinyl alcohol)-SiC nanofiber composite and its impact on mechanical properties: Positron annihilation and small-angle X-ray scattering studies. *Macromolecules*, 48(16): 5706-5713. <https://doi.org/10.1021/acs.macromol.5b01095>
- [2] Mahdi, S.M., Habeeb, M.A. (2022). Fabrication and tailored structural and dielectric characteristics of (SrTiO₃/NiO) nanostructure doped (PEO/PVA) polymeric blend for electronics fields. *Physics and Chemistry of Solid State*, 23(4): 785-792. <https://doi.org/10.15330/pcss.23.4.785-792>
- [3] Zhou, H.J., Rong, M.Z., Zhang, M.Q., Friedrich, K. (2006). Effects of reactive compatibilization on the performance of nano-silica filled polypropylene composites. *Journal of Materials Science*, 41: 5767-5770. <https://doi.org/10.1007/s10853-006-0112-x>
- [4] Metiab, M.H., Hashim, A., Rabee, B.H. (2023). Synthesis and structural properties of (PS-PC/Co2O3-

- SiC) nanocomposites for antibacterial applications. *Nanosistemi, Nanomateriali, Nanotehnologii*, 21(2): 451-460.
- [5] Elhosiny Ali, H., Abdel-Aziz, M., Mahmoud Ibrahim, A., Sayed, M.A., Abd-Rabboh, H.S., Awwad, N.S., Algarni, N., Shkir, M., Yasmin Khairy, M. (2022). Microstructure study and linear/nonlinear optical performance of Bi-embedded PVP/PVA films for optoelectronic and optical cut-off applications. *Polymers*, 14(9): 1741. <https://doi.org/10.3390/polym14091741>
- [6] Hayder, N., Hashim, A., Habeeb, M.A., Rabee, B.H., Hadi, A.G., Mohammed, M.K. (2022). Analysis of dielectric properties of PVA/PEG/ In_2O_3 nanostructures for electronics devices. *Revue des Composites et des Matériaux Avancés-Journal of Composite and Advanced Materials*, 32(5): 261-264. <https://doi.org/10.18280/rcma.320507>
- [7] Marten, F.L. (2002). Vinyl Alcohol Polymers. In *Encyclopedia of Polymer Science and Technology*. <https://doi.org/10.1002/0471440264.pst384>
- [8] Aso, O., Eguiazabal, J.I., Nazabal, J. (2007). The influence of surface modification on the structure and properties of a nanosilica filled thermoplastic elastomer. *Composites Science and Technology*, 67(13): 2854-2863. <https://doi.org/10.1016/j.compscitech.2007.01.021>
- [9] Akinay, Y., Kazici, H.C., Akkuş, I.N., Salman, F. (2021). Synthesis of 3D Sn doped Sb_2O_3 catalysts with different morphologies and their effects on the electrocatalytic hydrogen evolution reaction in acidic medium. *Ceramics International*, 47(20): 29515-29524. <https://doi.org/10.1016/j.ceramint.2021.07.278>
- [10] Condurache-Bota, S., Praisler, M., Gavrilă, R., Tigau, N. (2017). Sandwich heterostructures of antimony trioxide and bismuth trioxide films: Structural, morphological and optical analysis. *Applied Surface Science*, 391: 59-65. <https://doi.org/10.1016/j.apsusc.2016.07.033>
- [11] Tigau, N., Ciupina, V., Prodan, G., Rusu, G.I., Vasile, E. (2004). Structural characterization of polycrystalline Sb_2O_3 thin films prepared by thermal vacuum evaporation technique. *Journal of Crystal Growth*, 269(2-4): 392-400. <https://doi.org/10.1016/j.jcrysgro.2004.05.052>
- [12] Hadi, A.N., Abbas, T.M. (2024). Solvatochromic behavior on the absorption, transmittance and emission spectra for some organic dyes as active media. *Edelweiss Applied Science and Technology*, 8(6): 4026-4033.
- [13] Ge, S., Wang, Q., Shao, Q., Zhao, Y., Yang, X., Wang, X. (2011). Hydrothermal synthesis of morphology-controllable Sb_2O_3 microstructures: Hollow spindle-like and cobblestone-like microstructures. *Applied Surface Science*, 257(8): 3657-3665. <https://doi.org/10.1016/j.apsusc.2010.11.101>
- [14] Fan, G., Huang, Z., Chai, C., Liao, D. (2011). Synthesis of micro-sized Sb_2O_3 hierarchical structures by carbothermal reduction method. *Materials Letters*, 65(8): 1141-1144. <https://doi.org/10.1016/j.matlet.2010.09.084>
- [15] Honma, T., Sato, R., Benino, Y., Komatsu, T., Dimitrov, V. (2000). Electronic polarizability, optical basicity and XPS spectra of Sb_2O_3 - B_2O_3 glasses. *Journal of Non-Crystalline Solids*, 272(1): 1-13. [https://doi.org/10.1016/S0022-3093\(00\)00156-3](https://doi.org/10.1016/S0022-3093(00)00156-3)
- [16] Wang, X., Yang, Z., Mei, F., Zhou, Y., Xu, J., Jiang, Y. (2020). One pot synthesis of Sb_2O_3 /reduced graphene oxide composite anode material for sodium ion batteries. *Materials Letters*, 280: 128565. <https://doi.org/10.1016/j.matlet.2020.128565>
- [17] Obayes, H.K., Meteab, M.H., Al-Kareem, B.A. (2024). Modified dosimetric features of new type of lithium borate glass system: Role of magnesium and gold co-doping. *Transactions on Electrical and Electronic Materials*, 25(6): 708-721. <https://doi.org/10.1007/s42341-024-00551-2>
- [18] Hu, L., Qu, B., Chen, L., Li, Q. (2013). Low-temperature preparation of ultrathin nanoflakes assembled tremella-like NiO hierarchical nanostructures for high-performance lithium-ion batteries. *Materials Letters*, 108: 92-95. <https://doi.org/https://doi.org/10.1016/j.matlet.2013.06.060>
- [19] Xu, J., Kang, C., Niu, L., Xu, C., Ren, S. (2019). Study on the properties of the Sb_2O_3 nanoparticles modified by different surfactants. *Materials Research Express*, 6(9): 0950c1. <https://doi.org/10.1088/2053-1591/ab3563>
- [20] Yadav, A.A., Chavan, U.J. (2016). Influence of substrate temperature on electrochemical supercapacitive performance of spray deposited nickel oxide thin films. *Journal of Electroanalytical Chemistry*, 782: 36-42. <https://doi.org/10.1016/j.jelechem.2016.10.006>
- [21] Paulose, R., Mohan, R., Parihar, V. (2017). Nanostructured nickel oxide and its electrochemical behaviour—A brief review. *Nano-Structures & Nano-Objects*, 11: 102-111. <https://doi.org/10.1016/j.nanoso.2017.07.003>
- [22] Saca, N., Radu, L., Fugaru, V., Gheorghe, M., Petre, I. (2018). Composite materials with primary lead slag content: Application in gamma radiation shielding and waste encapsulation fields. *Journal of Cleaner Production*, 179: 255-265. <https://doi.org/10.1016/j.jclepro.2018.01.045>
- [23] Liu, H., Shi, J., Qu, H., Ding, D. (2019). An investigation on physical, mechanical, leaching and radiation shielding behaviors of barite concrete containing recycled cathode ray tube funnel glass aggregate. *Construction and Building Materials*, 201: 818-827. <https://doi.org/10.1016/j.conbuildmat.2018.12.221>
- [24] Zughbi, A., Kharita, M.H., Shehada, A.M. (2017). Determining optical and radiation characteristics of cathode ray tubes' glass to be reused as radiation shielding glass. *Radiation Physics and Chemistry*, 136: 71-74. <https://doi.org/10.1016/j.radphyschem.2017.02.035>
- [25] Mohammed, R.M., Habeeb, M.A., Hashim, A. (2020). Effect of antimony oxide nanoparticles on structural, optical and AC electrical properties of (PEO-PVA) blend for antibacterial applications. *International Journal of Emerging Trends in Engineering Research*, 8(8): 4726-4738. <https://doi.org/10.30534/ijeter/2020/107882020>
- [26] Rouhi, H.F., Aghaei, F., Kalangestani, F.C., Chenari, H.M., Nilkar, M. (2025). Enhanced electrocatalytic properties of plasma-treated MoS_2 - NiO -PVA nanofibers for hydrogen evolution reaction: A study of surface modifications and charge transfer kinetics. *Applied Surface Science*, 700: 163274. <https://doi.org/10.1016/j.apsusc.2025.163274>

- [27] Sopapan, P., Laopaiboon, J., Jaiboon, O., Yenchai, C., Laopaiboon, R. (2020). Feasibility study of recycled CRT glass on elastic and radiation shielding properties used as X-ray and gamma-ray shielding materials. *Progress in Nuclear Energy*, 119: 103149. <https://doi.org/10.1016/j.pnucene.2019.103149>
- [28] Zaidi, S.M.A., Kalyar, M.A., Raza, Z.A., Shoukat, A., Waseem, R., Aslam, M. (2024). Effect of laser irradiance on opto-electrical properties of PVA embedded graphene copper Ferrite nanocomposite strips. *Optical Materials*, 147: 114590. <https://doi.org/10.1016/j.optmat.2023.114590>
- [29] Saeed, A., Banoqitah, E., Abdulwahed, J.A.M., Alajmi, F., et al. (2024). A comprehensive study on structural, optical, electrical, and dielectric properties of PVA-PVP/Ag-TiO₂ nanocomposites for dielectric capacitor applications. *Journal of Alloys and Compounds*, 977: 173412. <https://doi.org/10.1016/j.jallcom.2023.173412>
- [30] Ragab, H.M., Diab, N.S., Khaled, A.M., Al Ojeery, A., Al-Hakimi, A.N., Farea, M.O. (2024). Incorporating hybrid Ag/Co₂O₃ nanofillers into PVP/CS blends for multifunctional optoelectronic and nanodielectric applications. *Ceramics International*, 50(1): 1254-1262. <https://doi.org/10.1016/j.ceramint.2023.10.219>
- [31] Issa, S.A., Zakaly, H.M.H., Pyshkina, M., Mostafa, M.Y.A., Rashad, M., Soliman, T.S. (2021). Structure, optical, and radiation shielding properties of PVA-BaTiO₃ nanocomposite films: An experimental investigation. *Radiation Physics and Chemistry*, 180: 109281. <https://doi.org/10.1016/j.radphyschem.2020.109281>
- [32] Zyoud, S.H., Almoadi, A., AlAbdulaal, T.H., Alqahtani, M.S., et al. (2023). Structural, optical, and electrical investigations of Nd₂O₃-doped PVA/PVP polymeric composites for electronic and optoelectronic applications. *Polymers*, 15(6): 1351. <https://doi.org/10.3390/polym15061351>
- [33] Mostafa, M.Y.A., Zakaly, H.M.H., Issa, S.A.M., Saudi, H.A., Henaish, A.M.A. (2022). Tailoring variations in the linear optical and radiation shielding parameters of PVA polymeric composite films doped with rare-earth elements. *Applied Physics A*, 128(3): 199. <https://doi.org/10.1007/s00339-022-05304-7>
- [34] Prakash, J., Jeyaram, S. (2022). Synthesis, characterization, morphological, linear and nonlinear optical properties of silicon carbide doped PVA nanocomposites. *Silicon*, 14(17): 11163-11170. <https://doi.org/10.1007/s12633-022-01852-y>
- [35] Jassim, H.H., Hashim, F.S. (2021). Synthesis of (PVA/PEG: ZnO and Co₃O₄) nanocomposites: Characterization and gamma ray studies. *NeuroQuantology*, 19(4): 47-56. <https://doi.org/10.14704/nq.2021.19.4.NQ21036>
- [36] Negim, E.S.M., Rakhmetullayeva, R.K., Yeligbayeva, G.Z., Urkimbaeva, P.I., Primzharova, S.T., Kaldybekov, D.B., Khatib, J.M., Mun, G.A., Craig, W. (2014). Improving biodegradability of polyvinyl alcohol/starch blend films for packaging applications. *International Journal of Basic and Applied Sciences*, 3(3): 263-273. <https://doi.org/10.14419/ijbas.v3i3.2842>
- [37] Olewnik-Kruszkowska, E., Gierszewska, M., Jakubowska, E., Tarach, I., Sedlarik, V., Pummerova, M. (2019). Antibacterial films based on PVA and PVA-chitosan modified with poly (hexamethylene guanidine). *Polymers*, 11(12): 2093. <https://doi.org/10.3390/polym11122093>
- [38] Bhadra, S., Khastgir, D. (2008). Determination of crystal structure of polyaniline and substituted polyanilines through powder X-ray diffraction analysis. *Polymer Testing*, 27(7): 851-857. <https://doi.org/10.1016/j.polymertesting.2008.07.002>
- [39] Mallapragada, S.K., Peppas, N.A., Colombo, P. (1997). Crystal dissolution-controlled release systems. II. Metronidazole release from semicrystalline poly(vinyl alcohol) systems. *Journal of Biomedical Materials Research*, 36(1): 125-130. [https://doi.org/10.1002/\(SICI\)1097-4636\(199707\)36:1<125::AID-JBM15>3.0.CO;2-H](https://doi.org/10.1002/(SICI)1097-4636(199707)36:1<125::AID-JBM15>3.0.CO;2-H)
- [40] Mansur, H.S., Sadahira, C.M., Souza, A.N., Mansur, A.A.P. (2008). FTIR spectroscopy characterization of poly (vinyl alcohol) hydrogel with different hydrolysis degree and chemically crosslinked with glutaraldehyde. *Materials Science and Engineering: C*, 28(4): 539-548. <https://doi.org/10.1016/j.msec.2007.10.088>
- [41] El-Kader, M.F.H.A., Elabbasy, M.T., Adeboye, A.A., Menazea, A.A. (2022). Nanocomposite of PVA/PVP blend incorporated by copper oxide nanoparticles via nanosecond laser ablation for antibacterial activity enhancement. *Polymer Bulletin*, 79(11): 9779-9795. <https://doi.org/10.1007/s00289-021-03975-5>
- [42] Abdali, K., Rabee, B.H., Al-Bermamy, E., Abdulridha, A.R., Abass, K.H., Kadim, A.M. (2023). Effect of doping Sb₂O₃NPs on morphological, mechanical, and dielectric properties of PVA/PVP blend film for electromechanical applications. *Nano*, 18(3): 2350011. <https://doi.org/10.1142/S179329202350011X>
- [43] Luo, Q., Shan, Y., Zuo, X., Liu, J. (2018). Anisotropic tough poly(vinyl alcohol)/graphene oxide nanocomposite hydrogels for potential biomedical applications. *RSC Advances*, 8(24): 13284-13291. <https://doi.org/10.1039/C8RA00340H>
- [44] Mohammed, M.K., Al-Dahash, G., Al-Nafiey, A. (2022). Fabrication and characterization of the PMMA/G/Ag nanocomposite by pulsed laser ablation (PLAL). *Nano Biomedicine and Engineering*, 14(1): 15-22. <https://doi.org/10.5101/nbe.v14i1.p15-22>
- [45] Pathan, H.M., Desai, J.D., Lokhande, C.D. (2002). Modified chemical deposition and physico-chemical properties of copper sulphide (Cu₂S) thin films. *Applied Surface Science*, 202(1-2): 47-56. [https://doi.org/10.1016/S0169-4332\(02\)00843-7](https://doi.org/10.1016/S0169-4332(02)00843-7)
- [46] Mohammed, M.K., Khudhair, T.N., Sharba, K.S., Hashim, A., Hadi, Q.M., Meteab, M.H. (2024). Tuning the morphological and optical characteristics of SnO₂/ZrO₂ nanomaterials doped PEO for promising optoelectronics applications. *Revue des Composites et des Matériaux Avancés-Journal of Composite and Advanced Materials*, 34(4): 495-503. <https://doi.org/10.18280/rcma.340411>
- [47] Sahib, S.R., Rabee, B.H. (2024). Production of a versatile PMMA/PEO-CuO-In₂O₃ nanocomposite with its characterization, cold plasma treatment, and applications for flexible emission filter devices and smart moisture. *Nano-Structures & Nano-Objects*, 40: 101382. <https://doi.org/10.1016/j.nano.2024.101382>
- [48] Aslam, M., Kalyar, M.A., Raza, Z.A. (2017). Graphene oxides nanosheets mediation of poly(vinyl alcohol) films in tuning their structural and opto-mechanical attributes.

- Journal of Materials Science: Materials in Electronics, 28(18): 13401-13413. <https://doi.org/10.1007/s10854-017-7177-y>
- [49] Sahib, S.R., Rabee, B.H. (2024). Synthesizing, characterizing, and cold plasma treating of $\text{Cr}_2\text{O}_3/\text{CuO}$ nanomaterials doped PMMA/PEO for flexible optoelectronic applications. *Optical Materials*, 157: 116139. <https://doi.org/10.1016/j.optmat.2024.116139>
- [50] Kadhim, W.K., Habeeb, M.A. (2024). Synthesis and tailoring the morphological, structural and optical characteristics of $\text{SiO}_2\text{-CO}_2\text{O}_3$ nanomaterials doped PVA-PEG for optoelectronic and food packing applications. *Optical and Quantum Electronics*, 56(8): 1346. <https://doi.org/10.1007/s11082-024-07275-w>
- [51] Zidan, H.M., Abdelrazek, E.M., Abdelghany, A.M., Tarabiah, A.E. (2019). Characterization and some physical studies of PVA/PVP filled with MWCNTs. *Journal of Materials Research and Technology*, 8(1): 904-913. <https://doi.org/10.1016/j.jmrt.2018.04.023>
- [52] Darwesh, A.H.A., Mohammed, P.A., Mamand, S.M., Hussien, S.A., Aziz, S.B., Brza, M.A., Abdullah, R.M., Karim, W.O. (2023). Investigation of structural and optical characteristics of biopolymer composites based on polyvinyl alcohol inserted with PbS nanoparticles. *Coatings*, 13(3): 578. <https://doi.org/10.3390/coatings13030578>
- [53] Al-abbas, S.S., Ghazi, R.A., Al-shammari, A.K., Aldulaimi, N.R., Abdulridha, A.R., Al-nesrawy, S.H., Al-bermany, E. (2021). Influence of the polymer molecular weights on the electrical properties of Poly (vinyl alcohol) – Poly (ethylene glycols)/ Graphene oxide nanocomposites. *Materials Today: Proceedings*, 42: 2469-2474. <https://doi.org/10.1016/j.matpr.2020.12.565>
- [54] A. Ejbarah, R., Khudhur Mohammed, M., Mohammed, A.J., Hashim, A. (2024). Studying the optical properties of nanocomposite PVA-PEG-ZrC. *Journal of Nanostructures*, 14(2): 427-436. <https://doi.org/10.22052/JNS.2024.02.006>
- [55] Soliman, T.S., Vshivkov, S.A., Elkalashy, S.I. (2020). Structural, thermal, and linear optical properties of SiO_2 nanoparticles dispersed in polyvinyl alcohol nanocomposite films. *Polymer Composites*, 41(8): 3340-3350. <https://doi.org/10.1002/pc.25623>
- [56] Fal, J., Bulanda, K., Traciak, J., Sobczak, J., Kuzioła, R., Grąz, K.M., Budzik, G., Oleksy, M., Żyła, G. (2020). Electrical and optical properties of silicon oxide lignin polylactide ($\text{SiO}_2\text{-L-PLA}$). *Molecules*, 25(6): 1354. <https://doi.org/10.3390/molecules25061354>
- [57] Jabber, A.A., Abdulridha, A.R. (2025). Preparation and characterization of CuO/ZnO nanostructures thin films using thermal evaporation for advanced gas sensing applications. *Trends in Sciences*, 22(3): 9002. <https://doi.org/10.48048/tis.2025.9002>
- [58] Abid, A.A., Al-Nesrawy, S.H., Abdulridha, A.R. (2021). New fabrication (PVA-PVP-C. B) nanocomposites: Structural and electrical properties. *Journal of Physics: Conference Series*, 1804(1): 012037. <https://doi.org/10.1088/1742-6596/1804/1/012037>
- [59] Dhaidan, F.M., Rabee, B.H. (2025). Fabrication and tailoring the microstructure and optical features of ($\text{PMMA-CoFe}_2\text{O}_4\text{-SiC}$) new nanostructures for photonics and radiation shielding applications. *Journal of Inorganic and Organometallic Polymers and Materials*. <https://doi.org/10.1007/s10904-025-03694-8>
- [60] Sattar, Z., Hashim, A. (2024). Fabrication and characteristics of PMMA-PEG/ $\text{SiO}_2\text{-SiC}$ quaternary nanocomposites for gamma ray shielding and flexible optoelectronics applications. *Journal of Materials Science: Materials in Electronics*, 35(24): 1660. <https://doi.org/10.1007/s10854-024-13435-1>
- [61] Sami, N.A., Nattah, A.M., Jawad, R.A., Meteab, M.H., Mohammed, M.K. (2025). Modification and enhancement of the structural, morphological and optical characteristics of PMMA/ $\text{In}_2\text{O}_3/\text{SiO}_2$ Promising Ternary Nanostructures for Optical Nanodevices and Gamma Ray Attenuation. *Trends in Sciences*, 22(7): 9959. <https://doi.org/10.48048/tis.2025.9959>
- [62] Rashad, M., Hanafy, T.A., Issa, S.A.M. (2020). Structural, electrical and radiation shielding properties of polyvinyl alcohol doped with different nanoparticles. *Journal of Materials Science: Materials in Electronics*, 31(18): 15192-15197. <https://doi.org/10.1007/s10854-020-04083-2>
- [63] Abdulsalam, H.S., Hashim, A., Mohammed, M.K. (2025). Synthesis and tuning the morphological and optical features of $\text{PS/SiO}_2\text{-Sb}_2\text{O}_3$ promising hybrid nanomaterials for radiation shielding and futuristic optoelectronics applications. *Journal of Materials Science: Materials in Electronics*, 36(8): 480. <https://doi.org/10.1007/s10854-025-14557-w>